processes

MDPI

Article

Examination of the Anti-Biofilm Properties of Lignocellulose-Based Activated Carbon from Black Alder for Water Treatment Applications

Irina Kandić [1], Milan Kragović [1], Jelena Gulicovski [1], Stefana Cvetković [2], Ana Marinković [1], Slaviša Stanković [2] and Marija Stojmenović [1,*]

[1] "Vinča" Institute of Nuclear Sciences—National Institute of the Republic of Serbia, University of Belgrade, 11351 Belgrade, Serbia; irina.kandic@vin.bg.ac.rs (I.K.); m.kragovic@vin.bg.ac.rs (M.K.); rocenj@vin.bg.ac.rs (J.G.); aradojevic@vin.bg.ac.rs (A.M.)

[2] Department of Microbiology, Faculty of Biology, University of Belgrade, Studentski trg 16, 11158 Belgrade, Serbia; stefana.cvetkovic@bio.bg.ac.rs (S.C.); slavisas@bio.bg.ac.rs (S.S.)

* Correspondence: mpusevac@vin.bg.ac.rs

Abstract: Nowadays, there is increasing global demand for activated carbon considering its wide usage as an adsorbent of environmental pollutants. Biowaste rich in lignocellulose, like the cone-like flowers of black alder (A_AC), shows promise as a precursor for novel materials. Building upon previous research and this material's established applicability for removing cyanobacteria cells and cyanotoxins from water, this study investigates the CNOHS composition of A_AC and its potential to inhibit biofilm formation. A comprehensive CNOHS analysis showed the material composition as 64.5%, 1.77%, 28.83%, 2.05%, and 0.12% for C, N, O, H, and S respectively. The material's efficacy in inhibiting biofilm formation across eight selected bacterial strains was evaluated. The results showed biofilm formation rates of 62.6%, 22.1%, 73.8%, 12.1%, 40.9%, 24.2%, 9.2%, and 7.6% for *Escherichia coli*, *Pseudomonas aeruginosa*, *Enterobacter cloacae*, *Salmonella* Typhimurium, *Proteus mirabilis*, *Klebsiella pneumoniae*, *Acinetobacter baumannii*, and *Enterococcus faecalis*, respectively. Biofilm formation is influenced by biotic and abiotic factors, especially the physicochemical properties of the substrate. This study offers insights into the potential of black-alder-derived activated carbon to prevent biofilm formation, highlighting its role in water purification and environmental protection.

Keywords: activated carbon; biowaste; biofilm; water treatment; eutrophic waters; sustainable materials

check for updates

Citation: Kandić, I.; Kragović, M.; Gulicovski, J.; Cvetković, S.; Marinković, A.; Stanković, S.; Stojmenović, M. Examination of the Anti-Biofilm Properties of Lignocellulose-Based Activated Carbon from Black Alder for Water Treatment Applications. *Processes* **2024**, *12*, 2383. https://doi.org/10.3390/pr12112383

Academic Editor: Anna Wołowicz

Received: 13 September 2024
Revised: 22 October 2024
Accepted: 25 October 2024
Published: 30 October 2024

Copyright: © 2024 by the authors. Licensee MDPI, Basel, Switzerland. This article is an open access article distributed under the terms and conditions of the Creative Commons Attribution (CC BY) license (https://creativecommons.org/licenses/by/4.0/).

1. Introduction

Water quality safety is closely related to human health, and microbes are one of the key factors affecting it [1]. Addressing microbial contamination sources is essential for maintaining water safety. Domestic sewage, hospital effluents, livestock waste, and landfill leachate contain numerous pathogenic microorganisms [2]. As key producers of organic matter in aquatic ecosystems, disruptions in the community structure or changes in the abundance of certain phytoplankton species, particularly toxin-producing cyanobacteria, can severely impact water quality in supply reservoirs and lead to acute or chronic health risks for plants, animals, and humans [3]. Eutrophication, rising nutrient levels, and anthropogenic activities lead to the proliferation of cyanobacteria, resulting in blooms in freshwater systems [4]. Common methods for water treatment include filtration, flocculation, reverse osmosis, and adsorption [5]. Adsorption processes are cost-effective, easy to operate, and highly efficient in water purification [6]. In adsorption-based wastewater treatment, organic and inorganic pollutants are drawn to the outer and inner surfaces of porous adsorbents through mass transfer and diffusion from the aqueous media to the adsorbent's active sites [5]. Activated carbon (AC), a carbon-rich solid produced from coal or biomass through thermal or thermochemical processes, is widely recognized as a good adsorbent, for its effectiveness in

water purification, particularly in removing a broad range of contaminants [7]. Among the contaminants that can be effectively removed by AC are dyes [8], herbicides [9], and heavy metals [10]. AC filters are particularly noteworthy due to their widespread use and ability to adsorb bacteria from water, which can then multiply on the filter and subsequently be released into the effluent [11]. The structure of the raw material significantly influences the porous structure and properties of carbonaceous adsorbents. The choice of precursor for activated carbon synthesis depends on its availability in nature, activation yield, and adsorption efficiency for pollutant removal. Therefore, selecting the right material is as important as choosing the production technology and optimizing processing conditions. Recently, there has been growing interest in using biomass waste from wood, food, and agriculture as novel sources for creating carbonaceous adsorbents [12]. Recent studies have highlighted that activated carbon derived from materials with a high lignocellulosic content, such as certain bio-wastes, demonstrates excellent performance [13]. The search for renewable and cost-effective alternatives for producing activated carbon from by-products and biomass residues has intensified recently. In Serbia, biomass is categorized into forest biomass (40%) and agricultural biomass (60%) based on burning convenience [14], with biowaste emerging as a key precursor in this process. Lignocellulosic biomasses are abundant, affordable, and possess properties ideal for developing sorbents [15]. One such promising bio-waste material is obtained from black alder cone-like flowers. Black alder is frequently used in the production of wooden floors, resulting in significant quantities of waste material that can be utilized for biochar production [16]. The species ranges from central Scandinavia to the Mediterranean, encompassing northern Morocco and Algeria, as well as northern Turkey, the Caucasus, and the Atlas Mountains valleys [17,18]. Activated carbon derived from black alder (A_AC) has been investigated for its efficacy in removing cyanobacteria and cyanotoxins from water. These initial studies indicate that the material works effectively for this purpose [19–21]. The A_AC exhibits no cytotoxicity towards MRC-5 cells, shows a concentration-dependent genotoxic response without significant effects at lower concentrations, and poses no significant health risk from heavy metals [21]. These findings provide critical insights into the safety and potential risks associated with A_AC, which are crucial for its applications and regulatory evaluations. The kinetics and mechanism of cyanobacteria cell removal are presented in the paper by Kandić et al. [21].

However, many factors can affect the performance and durability of AC in purification systems. One of those factors is biofilm formation which typically begins when organic nutrients are present in the surrounding environment, characteristic of eutrophic water. A biofilm is a collection of bacterial cells attached to a surface and encased in an extracellular matrix [22]. Different bacterial species can form distinct biofilm structures under identical conditions, and the same species may develop varying biofilm structures depending on environmental conditions [23]. Biofilm cells that are not embedded in a dense extracellular matrix may disperse more readily from the biofilm [22]. In drinking water distribution systems, biofilm formation can occur, causing various problems in water quality and safety due to the potential release of waterborne opportunistic pathogenic or pathogenic bacteria [24]. In nutrient-rich environments, the transition of bacterial cells from a planktonic to biofilm state becomes more pronounced, leading to denser biofilms [25]. Microorganisms within biofilms exhibit greater environmental resistance compared to free-floating microorganisms, enabling them to survive in harsh conditions [26]. They initially attach to the surface of the activated carbon. This attachment is facilitated by the physical properties of the activated carbon surface, such as its surface roughness, porosity, and specific surface area [27]. But we should bear in mind that AC is a non-selective adsorbent and there is the chance that cyanobacteria can be combined with the other microorganisms present in the water in a specific moment. This could be a positive effect because biofilms can enhance the removal of contaminants through synergistic interactions among different microorganisms, potentially improving the overall efficiency of the activated carbon in water treatment. To determine if this material has potential as a filter in contaminated water, it is essential

to investigate the potential for biofilm formation on its surface before it can be widely implemented in practical water treatment applications.

The suitable medium needs to have a high specific surface area, low cost, and a porosity high enough to avoid clogging and promote ventilation [25]. As presented in the paper by Kandić et al. [19], the A_AC has a specific surface 485 m^2/g and shows the presence of mesopores in addition to micropores in some percentages. In addition, the pores of the AC can remove particulate matter, allowing microorganisms to colonize, form biofilms, and proliferate by feeding on adsorbed organic matter, nutrients, and other microorganisms [28]. The detailed physical/chemical surface property of A_AC is presented in the paper by Kandić et al. [19]. Activated carbon surfaces typically contain various heteroatoms like oxygen, hydrogen, nitrogen, phosphorus, and sulfur, which form carbon-heteroatom structures derived from the starting material, with carbon–oxygen groups being the most common [29]. The ultimate analysis is showing percentage of C, N, O, H, and S in the material. The H/C ratio indicates aromaticity and O/C indicates hydrophilicity, while a (O + N)/C ratio indicates polarity [30]. The ratios of nutrient components within a system, rather than the nutrient components alone, may be significant in influencing biofilm development [31]. As biofilm formation is a major virulence factor for many microorganisms, it is increasingly important to gain a thorough understanding of this process. Most biofilm-associated infections are caused by the members of the family Enterobacteriaceae, with research primarily focusing on *Klebsiella pneumoniae* and *Salmonella* Typhimurium [32]. The material's efficacy was tested in biofilm formation experiments, building on its previous success in removing cyanobacteria and cyanotoxins [19–21]. We selected ultimate analysis to determine the elemental composition of the activated carbon (C, N, O, H, and S), which influences its adsorption properties and efficacy in inhibiting biofilm formation. Additionally, Raman spectroscopy was employed to provide detailed insights into the structural and molecular characteristics of the material, building on the results of the previously conducted FTIR analysis.

This article aims to provide a comprehensive understanding of the characteristics and potential applications of activated carbon derived from black alder cone-like flowers (A_AC) in mitigating the issue of potentially toxic cyanobacteria. The findings will contribute to assessing A_AC's suitability for practical water treatment applications, focusing on its structural properties, adsorption capabilities, and the impact of biofilm development on its long-term performance.

2. Materials and Methods

2.1. Material

The material examined in this study was activated carbon obtained from black alder (*Alnus glutinosa* L.) cone-like flowers. Firstly, the material was carbonized at 750 °C in a horizontal furnace. Secondly, it was activated at 750 °C in a CO_2 atmosphere, and it was labelled A_AC (Figure 1). The detailed parameters for the carbonization and activation processes, and characterization of material was previously described in a paper by Kandić et al. [19]. The list of abbreviations used in this article is provided in Table S1.

2.2. Ultimate Analysis of A_AC

The ultimate analysis of the synthesized A_AC was conducted to determine the elemental composition of carbon, hydrogen, nitrogen, sulfur, and oxygen. This analysis was performed using a LECO CHN 628 Series analyzer (LECO Corporation, St. Joseph, MI, USA) with a sulfur add-on module, following the standard test methods (ASTM, 2008, 2014) [33,34]. The oxygen content was calculated by difference, using the following formula: O = 100% − (ash + C + H + N + S).



Figure 1. Sample of activated carbon material obtained from black alder cone-like flowers (A_AC).

2.3. Raman Spectroscopy of A_AC

The Raman spectra for A_AC was recorded with a DXR Raman microscope (Thermo Scientific, Medison, WI, USA). Optical microscope and a CCD detector were used for a work of research. For measurement, we used an excitation wavelength of 532 nm. The scattered light was analyzed by the 900 lines mm^{-1} diffraction grating. The laser power was kept at 2.0 mW. The accumulation time for one spectrum was 10 s and 10 accumulations were collected for a single measurement. The spectrum was then averaged over three different sample areas. The automatic fluorescence correction was performed using the OMNIC software (latest v. 9.16).

2.4. Bacterial Strains

The following bacterial strains were tested: *Escherichia coli* ATCC 35218, *Pseudomonas aeruginosa* ATCC 27853, *Enterobacter cloacae* ATCC 49141, *Salmonella enterica* subsp. *enterica* serovar Typhimurium ATCC 14028, *Proteus mirabilis* ATCC 29906, *Klebsiella pneumoniae* ATCC 13885, *Acinetobacter baumannii* ATCC 19606, and *Enterococcus faecalis* ATCC 29219. The bacterial strains are the collection of Department of Microbiology, Faculty of Biology, University of Belgrade.

2.5. Effect of A_AC on Biofilm Formation

For antibiofilm testing, A_AC material was prepared in the following way: 200 mg of material was mixed with 2 mL of sterile distilled water. Prepared mixture was incubated for 24 h at 37 °C. After incubation, mixture was centrifuged (Heraeus Sepatech Medifuge, Hanau, Germany) for 10 min at 4000 rpm. Obtained supernatant was used in the following assays as 100% eluate.

2.5.1. Determination of Minimum Inhibitory Concentrations—MIC Assay

In order to determine the toxicity limit of A_AC, the MIC assay was conducted as previously described [35]. The MIC assay is based on making two-fold dilutions of test substances in 96-well plates. The A_AC was tested in concentrations ranging from 0.39% up to 50% and streptomycin was used as a positive control in concentrations ranging from 0.78 to 100 μg/mL. After the gradient of tested substances was created, in each well, bacterial inoculum (10^5 CFU/mL) and growth indicator resazurin (67.5 μg/mL) were added. The plates were wrapped with parafilm and incubated for 24 h at 37 °C.

2.5.2. Investigation of the Influence of A_AC on a Biofilm Formation

The effect of A_AC on preventing the process of biofilm formation was monitored by quantification of the total biofilm biomass, using crystal violet staining according to the method of Stepanović et al. [36], with slight modifications. The effect of A_AC on biofilm formation was tested on all the above mentioned bacterial strains. The method was performed in microtiter plates with 96 wells, where A_AC was tested in a concentration range 6.25–50%. On the first day, 50 µL of the bacterial suspension (10^6 CFU/mL) was added to the wells of the microtiter plate, and then 50 µL of the test substance of the appropriate concentration was added, contributing to a total volume of 100 µL. Selected concentrations of A_AC, as well as bacterial suspensions, were prepared in appropriate media with the addition of 0.5% glucose. The Mueller–Hinton broth (MHB) medium was used to test the effect on biofilm formation of *E. coli*, *P. aeruginosa*, *E. cloacae*, *K. pneumoniae*, and *S. Typhimurium*. For *E. faecalis* and *A. baumannii*, Luria-Bertani broth (LB) and Tryptic soy broth (TSB) medium were used, respectively. After setting up the experiment, the plates were incubated overnight (contact time was 24 h) at 37 °C. On the second day, the medium from the well was removed, the remaining contents were washed with water twice, and the plate was allowed to dry. After that, 100 µL of an aqueous solution of 0.1% crystal violet was added to each well and the plate was left to incubate for 20 min at room temperature. At the end of the incubation period, the plate was washed again with water and, after drying, absolute ethanol was added to dissolve the crystal violet that was bound to the biofilm mass. The total mass of the biofilm was determined by measuring the intensity of the crystal violet color at a wavelength of 570 nm (Multiscan FC, Thermo Scientific, Shanghai, China).

The percentage of inhibition of biofilm formation, compared to the untreated control, was calculated according to the following formula:

$$Inhibition\ of\ biofilm\ formation\ (\%) = 1 - \frac{A_t}{A_c} * 100$$

where A_t represents the mean absorbance of the treatment, while A_c represents the mean absorbance of the untreated control.

2.5.3. Statistical Analysis

Obtained data from antibiofilm studies were analyzed using GraphPad Prism 6.01 Software (Software, Inc., San Diego, CA, USA), and one-way ANOVA with Dunnet's and Tukey's post hoc tests was applied to test statistical significance at $p < 0.05$ level. For antibiofilm testing, three independent experiments with six wells per treatment were performed.

3. Results and Discussion

3.1. Ultimate Analysis of A_AC

The following Table 1 presents the ultimate analysis results and lignocellulose composition of the synthesized activated carbon material A_AC, in comparison with other available materials. Ultimate analysis, which includes the determination of elemental carbon, hydrogen, nitrogen, sulfur, and oxygen contents, provides information regarding the chemical composition and potential reactivity of the materials. Additionally, the lignocellulose composition is important for understanding the material's structural integrity and thermal stability.

Table 1. Ultimate analysis of A_AC and comparative materials, along with lignocellulose composition of precursors.

Material		A_AC	BAF	AG	PmS-B	SOC	WS	ATP	AS	OS
Reference		This study	[16] **	[37]	[30]	[13]	[38]	[38]	[38]	[38]
Ultimate analyses	C, %	64.5	74.8–89.3	44.4	71.8	44.5	45.1	51.3	50.5	44.8
	N, %	1.77	2.1–2.2	0.80	1.62	8.21	0.30	0.80	0.20	0.10
	O *, %	28.83	19.1–6.8	39.5	23.7	40.5	48.6	41.4	42.7	49.1
	H, %	2.05	4.00–1.70	2.05	2.91	6.28	6.00	6.50	6.60	6.00
	S, %	0.12	0.01	/	/	0.54	0.00	0.04	0.01	0.01
	H/C	0.03	0.63–0.23	0.05	0.04	0.14	0.13	0.13	0.13	0.13
	O/C	0.45	0.19–0.06	0.89	0.33	0.91	1.09	0.81	0.85	1.10
	(O + N)/C	0.47	0.28–0.10	0.91	0.35	1.09	1.08	0.82	0.85	1.10
Reference		[19]	[16]	[37]	[39]	[13]	[38]	[38]	[38]	[38]
Lignocellulose composition	Lignin, %	29.6	20.9	44.2	53.0	2.80	18.2	25.0	24.8	32.6
	Cellulose, %	19.1	29.7	14.2	29.5	21.6	40.1	33.7	32.5	30.8

* Calculated to 100%, the ash at 900 °C was 2.7% mass. ** Depending on the pyrolysis temperature (400–800 °C). BAF—biochar cone-like flowers; AG—Agricultural residues; PmS-B—biochar from waste plum stone; SOC—soybean oil cake; WS—walnut shell; ATP—almond tree pruning; AS—almond shell; OS—olive stone.

The comparison between A_AC, an activated carbon produced through a CO_2 activation process, and BAF [16], a biochar obtained via pyrolysis at temperatures ranging from 400 to 800 °C, offers valuable insights into how different synthesis methods impact the properties of materials derived from the same precursor. The key difference between these processes lies in the use of CO_2 for activation in the production of A_AC, whereas BAF is produced in an inert atmosphere. A_AC has a lower carbon content (64.5%) compared to BAF (74.8–89.3%). This implies that the activation process, although effective in functionalizing surfaces, may retain or introduce functional groups enhancing adsorption. In contrast, BAF's higher carbon content reflects more extensive carbonization, resulting in a denser, less reactive structure, potentially better suited for stable applications. Despite being an activated carbon, A_AC's carbon content, combined with its low ash content (2%), suggests a material has desirable characteristics for an adsorbent [40]. A_AC's nitrogen content (1.77%) is comparable to that of BAF (2.1–2.2%), implying that both materials retain nitrogenous functional groups, which can enhance adsorption through increased chemical reactivity [41]. The higher oxygen content in A_AC (28.83%) compared to BAF (6.8–19.1%) is particularly significant. The oxygen percentage reflects the concentration of oxygen-containing functional groups, which, in turn, indicates the material's surface hydrophilicity or hydrophobicity [42]. The activation process used for A_AC likely introduces more oxygenated functional groups, increasing the material's surface polarity and hydrophilicity. These properties make A_AC especially effective in removing polar compounds, making it suitable for high-activity applications like water purification [43,44]. The polar oxygen containing groups are mostly present in meso- or macropores, and non-polar groups are dominantly distributed on the surface of multilayer pores [30]. In the paper by Kandic et al. [19], A_AC is described to exhibit not only micropores but also a significant proportion of mesopores, indicating a diverse pore structure. In A_AC, the combination of micropores and mesopores with varying surface chemistries can enhance its ability to adsorb both polar and non-polar contaminants effectively. Moreover, the absence or minimal presence of sulfur in both A_AC and BAF highlights their eco-friendly nature, reinforcing the suitability of black alder cone-like flowers as a precursor for fabricating activated carbon [45]. This comparison shows that, while both A_AC and BAF have their

advantages, A_AC's activation process yields a material with a more functionalized, reactive surface, making it particularly well-suited for adsorption processes. The ultimate analysis of A_AC provides a clear view of how it compares to other biochars like AG (agricultural residues) [37], PmS-B (waste plum stone) [30], SOC (soybean oil cake) [13], WS (walnut shell) [38], ATP (almond tree pruning) [38], AS (almond shell) [38], and OS (olive stone) [38]. A_AC has a relatively high carbon content, making it more carbon-rich than AG, SOC, WS, and OS, but slightly less than PmS-B. The nitrogen content of A_AC aligns with PmS-B but much lower than the nitrogen-rich SOC and WS. The oxygen content in A_AC is higher than in PmS-B but it is much lower than in AG, SOC, WS, ATP, AS, and OS, reflecting the presence of oxygenated functional groups that enhance its reactivity.

The results were then used to calculate the H/C, O/C, and (O + N)/C ratios, which help in understanding the material's bonding and polarity. The lower H/C and O/C atomic ratios in A_AC confirm the occurrence of decarboxylation and dehydration during the synthesis [46]. Moreover, the value of H/C is an indicator of aromaticity, and lower values indicate a stable and stronger aromatic structure [15,30]. In the paper by Bakshi et al. [42], they propose that H/C molar ratios should be used as an index of stability in environmental modeling, as they are more accurate than O/C molar ratios, while the (O + N)/C ratio provide information about the amount of polar functional groups [30]. The A_AC's (O + N)/C ratio suggests a moderate presence of polar functional groups on its surface, which could enhance its ability to interact with polar molecules during adsorption processes.

Compared to other materials, A_AC exhibits moderate levels of carbonization and functional groups. The BAF, depending on its preparation conditions, shows varying degrees of carbonization with generally lower levels of oxygen and polar groups compared to A_AC. In contrast, AG, SOC, and WS have higher levels of oxygen and polar functional groups, making them more hydrophilic and reactive. Materials like PmS-B and AS fall in between, with moderate levels of functional groups and carbonization. OS has high levels of oxygen and polar groups, similar to SOC and WS. Overall, A_AC balances between high carbonization and moderate functionality, making it suitable for specific adsorption applications.

The high concentrations of C, O, and H are attributed to the nature of the three major structural polymers found in most lignocellulosic precursors: cellulose, hemicellulose, and lignin [47]. However, in this paper, only lignin and cellulose are specifically discussed. The content of lignocellulose in the precursor is crucial because the cross-linking between lignocellulose components determines the suitability of the biomass for activated carbon production. According to Ukanwa et al. [7], lignocellulosic biomass typically contains 10–30% lignin. It was also observed that materials with a higher lignin content result in a greater carbon yield, which is consistent with the findings from the lignocellulosic analysis [38]. In summary, black alder cone-like flowers have a lignin and cellulose composition that places it in the middle range compared to these materials. It is closer to BAF in cellulose content but higher in lignin compared to SOC and lower than AG. It also shows a balanced composition relative to ATP, AS, and OS. Concerning the activation process, cellulose exhibits the highest surface area and adsorption potential, with lignin following closely behind [48]. In this sense, black alder demonstrates significant potential for further research as a lignocellulose-rich precursor, especially in identifying suitable synthesis methods that can enhance its characteristics.

3.2. Raman Spectroscopy

The result of the Raman spectroscopy analysis of the activated form of black alder cone-like flowers (A_AC) is shown in Figure 2.

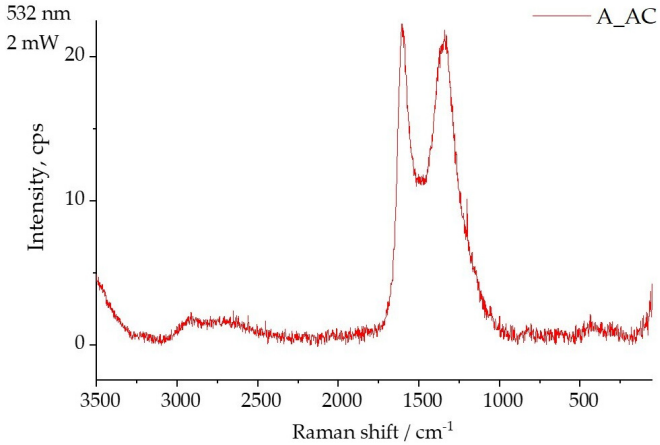

Figure 2. Raman spectroscopy analysis of A_AC.

In the material A_AC, peaks at 1606, 1340, and 1201 cm^{-1} can be observed. Two bands are clearly observed: D band at ~1340 cm^{-1}, which corresponds to the disordered structure of carbon, and G band at ~1600 cm^{-1}, which is bound and structured for graphite [49]. Connecting these findings, the presence of the G band in the Raman spectrum (at ~1606 cm^{-1}) aligns with the presence of aromatic C=C vibrations in the FTIR spectrum [19]. This indicates that both Raman and FTIR analyses confirm the graphitic nature and the presence of aromatic structures in the A_AC material. The D band in Raman (at ~1340 cm^{-1}) highlights the disordered structure within the carbon material, which may correlate with the reduced and simplified bands seen in the FTIR spectrum, signifying fewer complex organic structures remaining after activation [19].

3.3. Bacterial Strains and Their Impact on Human Health

For the inhibition of the biofilm formation of the test adsorbent A_AC, eight bacterial strains were selected—*Escherichia coli*, *Pseudomonas aeruginosa*, *Enterobacter cloacae*, *Salmonella* Typhimurium, *Proteus mirabilis*, *Klebsiella pneumoniae*, *Acinetobacter baumannii*, and *Enterococcus faecalis.* The characteristics are presented in Table 2. These bacterial strains were chosen due to their relevance as common pathogens and their potential to form biofilms in aquatic environments.

Table 2. Overview of bacterial characteristics and pathogenicity.

Bacteria	Family	Gram Staining	Oxygen Demand
Escherichia coli	Enterobacteriaceae	Gram-negative	Facultative anaerobic
Pseudomonas aeruginosa	Pseudomonadaceae	Gram-negative	Facultative anaerobic
Enterobacter cloacae	Enterobacteriaceae	Gram-negative	Facultative anaerobic
Salmonella Typhimurium	Enterobacteriaceae	Gram-negative	Facultative anaerobic
Proteus mirabilis	Enterobacteriaceae	Gram-negative	Facultative anaerobic
Klebsiella pneumoniae	Enterobacteriaceae	Gram-negative	Facultative anaerobic
Acinetobacter baumannii	Moraxellaceae	Gram-negative	Aerobic
Enterococcus faecalis	Enterococcaceae	Gram-positive	Facultative anaerobic

Those bacteria are ubiquitous in the environment, shaping ecosystems and impacting the health of other organisms and playing critical roles such as nutrient cycling by decomposing organic matter and releasing essential elements [50]. Facultative anaerobes can grow with or without oxygen, allowing them to thrive in various environments and adapt to changing conditions, giving them a selective advantage over other bacteria [51]. Unlike facultative anaerobes, aerobic bacteria are strictly dependent on oxygen for their growth and metabolism. Facultative anaerobes, in that way, have a selective advantage due to their adaptability to various environments. There are two major groups of bacteria: Gram-positive and Gram-negative bacteria. Gram-negative bacteria have a thin peptidoglycan cell

wall and an outer membrane with lipopolysaccharides. In contrast, Gram-positive bacteria lack an outer membrane but have a much thicker peptidoglycan layer. Gram-negative bacteria are predominant, similar to their prevalence in water distribution systems [11]. *E. coli*, a common pathogen causing diarrhea in humans and animals, can easily form biofilms on various surfaces [26]. *P. aeruginosa* is an opportunistic bacterial pathogen and a major cause of hospital-acquired infections [52]. *E. cloacae* is known for causing infections by forming biofilms on various abiotic surfaces [32]. *S*. Typhimurium belongs to the *Salmonella* genus, a prevalent and widely distributed bacterial pathogen responsible for causing salmonellosis [22]. *P. mirabilis* is commonly found in diverse environments such as soil, water sources, and sewage, but it primarily resides as a commensal organism in the gastrointestinal tracts of humans and animals [53]. *K. pneumoniae* is a major cause of human infections and a leading global concern for multi-drug resistant (MDR) microorganisms, utilizing a variety of virulence factors [54]. It is found mainly in the form of adherent biofilms rather than free-floating planktonic cells [55]. *A. baumannii* is an opportunistic pathogen predominantly linked to hospital-acquired infections [56]. *E. faecalis* is commonly detected in natural water and is typically found in the intestines of humans and animals, with a detection rate in feces that ranks just below that of *E. coli* [1]. Given their widespread presence and impact on human and animal health, these bacteria are suitable candidates for biofilm experiments on A_AC. This material will further be used for the removal of cyanobacteria cells from a eutrophic lake.

3.4. The Minimum Inhibitory Concentrations—MIC Assay

The results of the microdilution method showed that the tested material, within a certain concentration range, did not exhibit an inhibitory effect. Even though the A_AC did not show any inhibitory potential, i.e., the MICs were not determined in the microdilution assay, the investigation of the antibiofilm effect continued, given that the mechanisms of inhibitory and antibiofilm effects are different. If a tested agent does not inhibit bacterial growth, it does not exclude its ability to reduce or inhibit biofilm formation through mechanisms such as the inhibition of quorum sensing, initial adhesion, or extracellular matrix synthesis [57].

3.5. The Effect of A_AC on the Inhibition of Biofilm Formation

The effect of A_AC on the inhibition of biofilm formation is shown in Figure 3. The chart shows the extent to which A_AC reduces or prevents the growth of biofilms compared to the control samples.

The results of the study on the antibiofilm effect of A_AC on eight bacterial strains reveal significant variability in bacterial susceptibility. The data indicate that *Escherichia coli* and *Enterobacter cloacae* exhibit a high sensitivity to A_AC, particularly at higher concentrations, with inhibition rates reaching 62.6% and 73.8%, respectively, at a 50% concentration. This inhibition suggests that A_AC could be highly effective in reducing these bacteria in contaminated water, highlighting its potential utility in water treatment applications. Conversely, *Pseudomonas aeruginosa* and *Salmonella* Typhimurium show markedly lower inhibition rates across all tested concentrations, with a maximum inhibition of 22.1% and 12.1%, respectively, at a 50% concentration.

Similarly, in the case of *Acinetobacter baumannii* and *Enterococcus faecalis*, the minimal inhibition of biofilm formation was recorded, not exceeding 10% even at the highest concentration. These results suggest that these strains possess resistance mechanisms that mitigate the effectiveness of A_AC, pointing to a limitation in the broad-spectrum applicability of this material. The inhibition of *Proteus mirabilis* and *Klebsiella pneumoniae* increases gradually with concentration, achieving moderate levels at the highest concentration (40.9% and 24.2%, respectively). This indicates a concentration-dependent response, where higher doses of A_AC are required to achieve significant antibacterial effects.

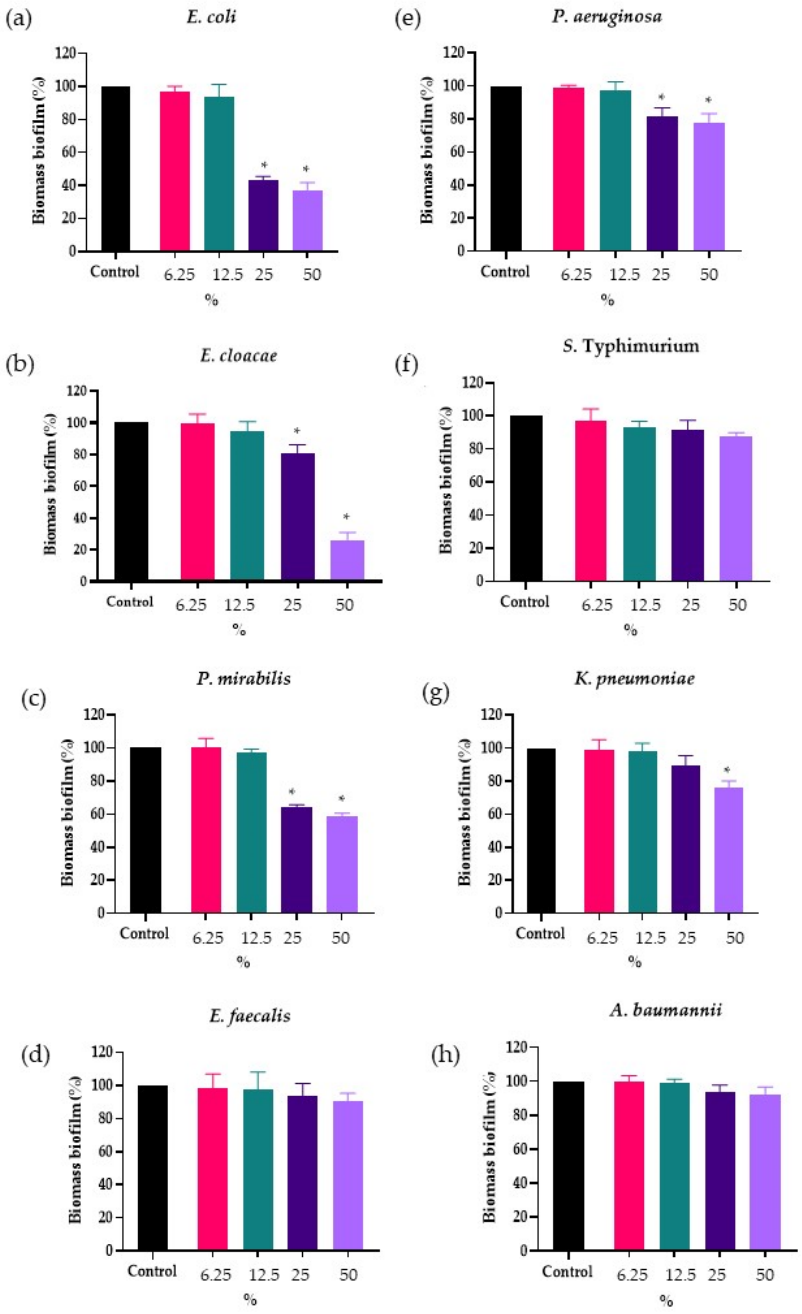

Figure 3. The inhibition on formation of biofilm for bacterial strains: (**a**) *E. coli*, (**b**) *P. aeruginosa*, (**c**) *E. cloacae*, (**d**) *S.* Typhimurium, (**e**) *P. mirabilis*, (**f**) *K. pneumoniae*, (**g**) *A. baumannii*, and (**h**) *E. faecalis.* Statistical significance with regard to untreated control was tested using one-way ANOVA with Dunnet's post hoc test (* $p < 0.05$).

The results, in general, present that A_AC shows the antibiofilm effect towards *E. coli* and *E. cloacae*, followed by *P. mirabilis* and *K. pneumoniae*. Biofilms formed by *E. coli* on surfaces in aquatic environments, such as sediments, are a well-documented factor contributing to the persistence of *E. coli* in natural settings [58]. However, the A_AC exhibited an anti-biofilm effect on *E. coli*. Research by Zhou et al. [26] has shown that calcite exhibits broad-spectrum antibacterial properties against *E. coli*. The presence of calcite in material A_AC has been confirmed by XRD analysis [19] which can be one of the reasons for this result. In the research by Reasoner [59], the absence of *E. coli* and *E. cloacae* biofilm on the activated carbon filters has been shown and they were undetectable in the product water following the initial sample. The anti-biofilm effect observed at

high concentrations of A_AC might be linked to its ability to induce oxidative stress in *K. pneumoniae*, which disrupts biofilm formation [60]. This oxidative stress likely impairs the bacteria's ability to maintain a stable biofilm, making A_AC an effective material for inhibiting *K. pneumoniae* biofilm development. The absence of biofilm formation on A_AC can be attributed to its broad-spectrum inhibitory effects against *P. mirabilis*, which may play a role in controlling biofilm-associated infectious diseases in aquatic environments [61]. On the other hand, the lack of an A_AC antibiofilm effect was observed for the remaining bacteria. *S.* Typhimurium undergoes genetic and physiological changes known as the starvation-stress response due to carbon deficits, with a similar but less extensive response to phosphate or nitrogen deprivation, and this process is significantly influenced by environmental conditions like temperature and the strain's origin [22,62]. This advantage arises from the material's carbon richness, which promotes biofilm development, with a smaller contribution from the nitrogen present (Table 1). The environmental sample screening identified *P. aeruginosa* as significantly associated with hydrocarbon-contaminated environments, unlike uncontaminated areas where its prevalence was low [52]. The 64.5% carbon content in material A_AC likely promotes biofilm formation by *P. aeruginosa*, providing a favorable surface for adhesion and growth. Additionally, the porous structure of A_AC offers protection and a nutrient-rich environment, further enhancing biofilm development. Results for *A. baumannii* are in accordance with the fact that it is challenging to break the biofilm once formed on surfaces due to its resistance and tendency to survive in nutrient-free environments [63]. Further on, nutrient levels affect *E. faecalis* biofilm development, with rich conditions producing regular biofilms and limited nutrients leading to irregular biofilms [64]. In that sense, A_AC is a suitable medium for its growth because it provides the essential nutrients and supports the conditions needed for optimal biofilm formation, allowing *E. faecalis* to thrive and develop effectively.

The inhibition percentages of biofilm formation at different concentrations (6.25%, 12.5%, 25%, and 50%) of A_AC are presented in Table 3. The inhibition percentages are accompanied by standard deviations and statistical significance. A statistical analysis reveals significant differences among inhibition rates, particularly at higher concentrations of A_AC. This variance underscores the necessity for optimized dosages in treatment protocols, as higher concentrations significantly enhance the biofilm inhibitory effects, especially against *E. cloacae* and *E. coli*.

Table 3. Inhibitions of biofilm formation after the treatment with A_AC.

Concentration	6.25%	12.5%	25%	50%
Strains	**Inhibition (%)**			
E. coli	2.8 ± 2.9^{a}	6.4 ± 7.7^{a}	56.6 ± 2.1^{a}	62.6 ± 4.3^{a}
P. aeruginosa	0.9 ± 1.3^{a}	2.9 ± 5.3^{a}	18.3 ± 5.2^{b}	22.1 ± 5.3^{b}
E. cloacae	0.7 ± 6.2^{a}	5.6 ± 6.3^{a}	19.6 ± 5.9^{b}	73.8 ± 4.8^{c}
S. Typhimurium	2.9 ± 7.1^{a}	6.8 ± 3.5^{a}	8.3 ± 5.7^{b}	12.1 ± 2.1^{d}
P. mirabilis	0.5 ± 4.7^{a}	2.8 ± 2.1^{a}	35.7 ± 1.5^{c}	40.9 ± 1.7^{e}
K. pneumoniae	1.3 ± 6.6^{a}	1.6 ± 4.7^{a}	10.4 ± 5.9^{b}	24.2 ± 4.4^{b}
E. faecalis	1.5 ± 8.5^{a}	2.2 ± 10.1^{a}	6.1 ± 7.3^{b}	9.2 ± 4.5^{d}
A. baumannii	0.3 ± 3.6^{a}	1.3 ± 2.6^{a}	6.2 ± 4.1^{b}	7.6 ± 4.3^{d}

The results are presented as mean values ± standard deviation. Statistical significance was analyzed by one-way ANOVA, using Tukey's post hoc test. Each different letter in a column indicates statistical significance between tested bacterial strains at that concentration level.

The formation of biofilm on a surface can influence, both positively and negatively, the performances of materials, specifically the material used as an adsorbent. The positive aspect of biofilm formation is the possible facilitation of the removal of cyanobacteria along with other microorganisms, including potential pathogens, from the water. Conversely, a negative impact is that, if the tested bacteria do not co-form biofilms with cyanobacteria, they may compete for the limited available pores on A_AC. A major limitation of AC, in general, is organic matter saturation, which leads to exhausted media that allow

contaminants to pass through, potentially causing water quality issues and promoting bacterial regrowth in distribution systems [28]. Furthermore, species such as *E. coli*, *E. cloacae*, *P. mirabilis*, and *K. pneumoniae* showed a susceptibility to A_AC, suggesting that this material could inhibit the initial biofilm formation of these species, thereby minimizing the risk of post-treatment water contamination. The variability in biofilm inhibition rates underscores the necessity for further studies to explore the underlying mechanisms of bacterial resistance and the potential for enhancing the antibacterial efficacy of A_AC. The formation of biofilms on its surface remains an important consideration for its long-term use in water treatment.

The structural properties of A_AC, such as pore size distribution and surface chemistry, play a crucial role in its performance for both biofilm inhibition and adsorption. As presented in the study by Kandić et al. [19], A_AC possesses a specific surface area and includes both micropores and mesopores. This combination of pore types contributes significantly to the material's functionality in water treatment applications. However, while these pores are effective in adsorbing organic matter and particulate materials, they also create an environment conducive to the colonization of microorganisms. This can provide an explanation of the biofilm formation of the analyzed bacterial strains on the material's surface. This duality underscores the importance of optimizing the pore structure and surface chemistry of A_AC to balance its adsorption capabilities with its effectiveness in inhibiting biofilm formation.

The biofilm inhibition results in Table 3 reflect the complex interplay between the material's adsorption properties and its impact on microbial activity. Although A_AC demonstrated promising inhibition effects, particularly against *E. coli* and *E. cloacae*, the formation of biofilms can still be facilitated by the availability of adsorbed nutrients within the material's pores. Understanding this relationship is essential for further improving the material's design to enhance both adsorption efficiency and antimicrobial properties, making it a more effective tool in water treatment. Further insight into the in situ biofilm formation on A_AC and its characteristics is needed and is part of future research. However, those are valuable results for better understanding this specific material and can be implemented in water treatment applications and will contribute to new knowledge in the field.

4. Conclusions

In this study, anti-biofilm properties, and the application of activated carbon derived from natural precursors, were examined for the removal of cyanobacterial cells from water resources. The activated carbon material A_AC, obtained from the conical flowers of black alder, shows a promising balance of high carbon content and functionalized surface features, making it effective for adsorption applications. The results showed an inhibition of biofilm formation of 62.6%, 22.1%, 73.8%, 12.1%, 40.9%, 24.2%, 9.2%, and 7.6% for *Escherichia coli*, *Pseudomonas aeruginosa*, *Enterobacter cloacae*, *Salmonella* Typhimurium, *Proteus mirabilis*, *Klebsiella pneumoniae*, *Acinetobacter baumannii*, and *Enterococcus faecalis*, respectively. The significant inhibition of biofilm formation, especially against *E. coli* and *E. cloacae*, suggests that A_AC possess a good potential utility in water treatment. However, the variability in its efficacy between different bacterial strains highlights the need for further optimization and detailed characterization. Additionally, the potential leaching of material during water treatment processes presents another important aspect that warrants closer examination. Leaching could not only reduce the efficiency of the activated carbon but may also introduce undesirable components into treated water, which could impact environmental and human health. Future research should focus on refining the surface properties of A_AC, examining its performance under different environmental conditions, and thoroughly assessing its environmental impact. Such studies will improve our understanding of the practical applications and limitations of A_AC, ultimately contributing to more efficient, safer, and sustainable water treatment solutions.

Supplementary Materials: The following supporting information can be downloaded at: https://www.mdpi.com/article/10.3390/pr12112383/s1, Table S1: List of abbreviation and full name/description.

Author Contributions: Conceptualization, M.S., S.S. and I.K.; investigation, M.S. and I.K.; methodology, M.K., J.G. and S.C.; validation, I.K. and M.S.; formal analysis, M.K., J.G., A.M. and S.C.; writing–original draft, I.K. and M.S.; writing–review and editing, M.S. and M.K.; super-vision, M.S., S.S. and M.K. All authors have read and agreed to the published version of the manuscript.

Funding: This research received no external funding.

Data Availability Statement: Data are contained within the article and Supplementary Materials.

Acknowledgments: These investigations were supported by the Ministry of Education, Science, and Technological Development of the Republic of Serbia (Contract numbers 451-03-66/2024-03/200017 through the realization of research themes 1702403 and 1702405, and 451-03-65/2024-03/200178). We would like to thank the Danica Bajuk-Bogdanović, Faculty of Physical Chemistry, University of Bel-grade, Studentski Trg 12-16, Belgrade 11158, Serbia for the Raman spectra determination.

Conflicts of Interest: The authors declare no conflicts of interest.

References

1. Yu, J.; Zhang, D.; Ren, W.; Liu, B. Transport of Enterococcus faecalis in granular activated carbon column: Potential energy, migration, and release. *Colloids Surf. B Biointerfaces* **2019**, *183*, 110415. [CrossRef] [PubMed]
2. Bradford, S.A.; Morales, V.L.; Zhang, W.; Harvey, R.W.; Packman, A.I.; Mohanram, A.; Welty, C. Transport and fate of microbial pathogens in agricultural settings. *Crit. Rev. Environ. Sci. Technol.* **2013**, *43*, 775–893. [CrossRef]
3. Zlatković, S.; Medić, O.; Predojević, D.; Nikolić, I.; Subakov-Simić, G.; Onjia, A.; Berić, T.; Stanković, S. Spatio-temporal dynamics in physico-chemical properties, phytoplankton and bacterial diversity as an indication of the Bovan reservoir water quality. *Water* **2022**, *14*, 391. [CrossRef]
4. Kulabhusan, P.K.; Campbell, K. Physio-chemical treatments for the removal of cyanotoxins from drinking water: Current challenges and future trends. *Sci. Total Environ.* **2024**, *917*, 170078. [CrossRef]
5. Karume, I.; Bbumba, S.; Tewolde, S.; Mukasa, I.H.Z.; Ntale, M. Impact of carbonization conditions and adsorbate nature on the performance of activated carbon in water treatment. *BMC Chem.* **2023**, *17*, 162. [CrossRef] [PubMed]
6. Najdanović, S.M.; Petrović, M.M.; Kostić, M.M.; Velinov, N.D.; Radović Vučić, M.D.; Matović, B.Ž.; Bojić, A.L. New way of synthesis of basic bismuth nitrate by electrodeposition from ethanol solution: Characterization and application for removal of RB19 from water. *Arab. J. Sci. Eng.* **2019**, *44*, 9939–9950. [CrossRef]
7. Ukanwa, K.S.; Patchigolla, K.; Sakrabani, R.; Anthony, E.; Mandavgane, S. A review of chemicals to produce activated carbon from agricultural waste biomass. *Sustainability* **2019**, *11*, 6204. [CrossRef]
8. Boudechiche, N.; Fares, M.; Ouyahia, S.; Yazid, H.; Trari, M.; Sadaoui, Z. Comparative study on removal of two basic dyes in aqueous medium by adsorption using activated carbon from Ziziphus lotus stones. *Microchem. J.* **2019**, *146*, 1010–1018. [CrossRef]
9. Bojić, D.V.; Kostić, M.M.; Radović-Vučić, M.D.; Velinov, N.D.; Najdanović, S.M.; Petrović, M.M.; Bojić, A.L. Removal of the herbicide 2, 4-dichlorophenoxyacetic acid from water by using an ultrahighly efficient thermochemically activated carbon. *Chem. Ind.* **2019**, *73*, 223–237. [CrossRef]
10. Melliti, A.; Yılmaz, M.; Sillanpää, M.; Hamrouni, B.; Vurm, R. Low-cost date palm fiber activated carbon for effective and fast heavy metal adsorption from water: Characterization, equilibrium, and kinetics studies. *Colloids Surf. A Physicochem. Eng. Asp.* **2023**, *672*, 131775. [CrossRef]
11. Dufour, A.P. Health studies of aerobic heterotrophic bacteria colonizing granular activated carbon systems. In Proceedings of the 9S: Conference on Point-of-Use Treatment of Drinking Water, Cincinnati, OH, USA, 6–8 October 1987; p. 84.
12. Ganjoo, R.; Sharma, S.; Kumar, A.; Daouda, M.M. Activated carbon: Fundamentals, classification, and properties. In *Activated Carbon: Progress and Applications*; Royal Society of Chemistry: London, UK, 2023. [CrossRef]
13. Tay, T.; Ucar, S.; Karagöz, S. Preparation and characterization of activated carbon from waste biomass. *J. Hazard. Mater.* **2009**, *165*, 481–485. [CrossRef] [PubMed]
14. Marinković, A.; Repić, B.; Spasojević, V.; Mladenović, M.; Đurović, D. Određivanje karakteristika agro i šumske biomase u cilju njihove energetske primene. *Savrem. Poljopr. Teh.* **2015**, *41*, 197–204. [CrossRef]
15. Lopičić, Z.; Avdalović, J.; Milojković, J.; Antanasković, A.; Lješević, M.; Lugonja, N.; Šoštarić, T. Removal of diesel pollution by biochar-support in water remediation. *Chem. Ind.* **2021**, *75*, 329–339. [CrossRef]
16. Mokrzycki, J.; Gazińska, M.; Fedyna, M.; Karcz, R.; Lorenc-Grabowska, E.; Rutkowski, P. Pyrolysis and torrefaction of waste wood chips and cone-like flowers derived from black alder (*Alnus glutinosa* L. Gaertn.) for sustainable solid fuel production. *Biomass Bioenergy* **2020**, *143*, 105842. [CrossRef]
17. Kajba, D.; Gracan, J. *EUFORGEN Technical Guidelines for Genetic Conservation and Use for Black Alder (Alnus glutinosa)*; Bioversity International: Roma, Italy, 2003.

18. Claessens, H.; Oosterbaan, A.; Savill, P.; Rondeux, J. A review of the characteristics of black alder (*Alnus glutinosa* (L.) Gaertn.) and their implications for silvicultural practices. *Forestry* **2010**, *83*, 163–175. [CrossRef]
19. Kandić, I.; Kragović, M.; Krstić, J.B.; Gulicovski, J.; Popović, J.; Rosić, M.; Karadžić, V.; Stojmenović, M. Natural Cyanobacteria Removers Obtained from Bio-Waste Date-Palm Leaf Stalks and Black Alder Cone-Like Flowers. *Int. J. Environ. Res. Public Health* **2022**, *19*, 6639. [CrossRef]
20. Kandić, I.; Kragović, M.; Gulicovski, J.; Nikolić, K.; Nišić, N.; Karadžić, V.; Stojmenović, M. Removal of potentially toxic cyanobacteria by using activated carbons obtained from biowaste. In *MEP-23: 9th International Conference Mining and Environmental Protection: Proceedings Book*; Faculty of Mining and Geology, University of Belgrade: Belgrade, Serbia, 2023; pp. 286–290.
21. Kandić, I.; Kragović, M.; Živković, S.; Knežević, J.; Vuletić, S.; Cvetković, S.; Stojmenović, M. Kinetics and Mechanism of Cyanobacteria Cell Removal Using Biowaste-Derived Activated Carbons with Assessment of Potential Human Health Impacts. *Toxins* **2024**, *16*, 310. [CrossRef]
22. Castelijn, G.A.; van der Veen, S.; Zwietering, M.H.; Moezelaar, R.; Abee, T. Diversity in biofilm formation and production of curli fimbriae and cellulose of Salmonella Typhimurium strains of different origin in high and low nutrient medium. *Biofouling* **2012**, *28*, 51–63. [CrossRef]
23. Tolker-Nielsen, T. Biofilm development. In *Microbial Biofilms*; John Wiley & Sons, Inc.: Hoboken, NJ, USA, 2015; pp. 51–66.
24. Erdei-Tombor, P.; Kiskó, G.; Taczman-Brückner, A. Biofilm Formation in Water Distribution Systems. *Processes* **2024**, *12*, 280. [CrossRef]
25. Sehar, S.; Naz, I. Role of the biofilms in wastewater treatment. In *Microbial Biofilms: Importance and Applications*; InTech: London, UK, 2016; pp. 121–144.
26. Zhou, F.; Wang, D.; Hu, J.; Zhang, Y.; Tan, B.K.; Lin, S. Control measurements of Escherichia coli biofilm: A review. *Foods* **2022**, *11*, 2469. [CrossRef]
27. Murshid, S.; Antonysamy, A.; Dhakshinamoorthy, G.; Jayaseelan, A.; Arivalagan, P. A review on biofilm-based reactors for wastewater treatment: Recent advancements in biofilm carriers, kinetics, reactors, economics, and future perspectives. *Sci. Total Environ.* **2023**, *892*, 164796. [CrossRef] [PubMed]
28. Simpson, D.R. Biofilm processes in biologically active carbon water purification. *Water Res.* **2008**, *42*, 2839–2848. [CrossRef] [PubMed]
29. Considine, R.; Denoyel, R.; Pendleton, P.; Schumann, R.; Wong, S.H. The influence of surface chemistry on activated carbon adsorption of 2-methylisoborneol from aqueous solution. *Colloids Surf. A Physicochem. Eng. Asp.* **2001**, *179*, 271–280. [CrossRef]
30. Lopičić, Z.R.; Šoštarić, T.D.; Milojković, J.V.; Antanasković, A.V.; Milić, J.S.; Spasić, S.D.; Avdalović, J.S. Efficient Removal of Water Soluble Fraction of Diesel Oil by Biochar Sorption Supported by Microbiological Degradation. *Processes* **2024**, *12*, 964. [CrossRef]
31. Thompson, L.J.; Gray, V.; Lindsay, D.; Von Holy, A. Carbon: Nitrogen: Phosphorus ratios influence biofilm formation by Enterobacter cloacae and Citrobacter freundii. *J. Appl. Microbiol.* **2006**, *101*, 1105–1113. [CrossRef]
32. Misra, T.; Tare, M.; Jha, P.N. Insights into the dynamics and composition of biofilm formed by environmental isolate of Enterobacter cloacae. *Front. Microbiol.* **2022**, *13*, 877060. [CrossRef]
33. *ASTM D5016-08*; Standard Test Method for Total Sulfur in Coal and Coke Combustion Residues Using a High-Temperature Tube Furnace Combustion Method with Infrared Absorption. ASTM: West Conshohocken, PA, USA, 2008.
34. *ASTM D5373-14*; Standard Test Methods for Determination of Carbon, Hydrogen and Nitrogen in Analysis Samples of Coal and Carbon in Analysis Samples of Coal and Coke. ASTM: West Conshohocken, PA, USA, 2014.
35. Cvetković, S.; Tenji, D.; Mitić-Ćulafić, D.; Vuletić, S.; Ganić, T.; Djekić, I.; Nikolić, B. Potential of yellow gentian aqueous-ethanolic extracts to prevent Listeria monocytogenes biofilm formation on selected food contact surfaces. *Food Biosci.* **2023**, *54*, 102857. [CrossRef]
36. Stepanović, S.; Vuković, D.; Dakić, I.; Savić, B.; Švabić-Vlahović, M. A modified microtiter-plate test for quantification of staphylococcal biofilm formation. *J. Microbiol. Methods* **2000**, *40*, 175–179. [CrossRef]
37. Sun, X.; Shan, R.; Li, X.; Pan, J.; Liu, X.; Deng, R.; Song, J. Characterization of 60 types of Chinese biomass waste and resultant biochars in terms of their candidacy for soil application. *Gcb Bioenergy* **2017**, *9*, 1423–1435. [CrossRef]
38. González, J.F.; Román, S.; Encinar, J.M.; Martínez, G. Pyrolysis of various biomass residues and char utilization for the production of activated carbons. *J. Anal. Appl. Pyrolysis* **2009**, *85*, 134–141. [CrossRef]
39. Lendler, M. Mogućnosti Korištenja Industrijskih Ostataka Važnijeg Koštuničavog voća Procesom Pirolize u Svrhu Dobivanja Energije. Doctoral Dissertation, Department of Agricultural Technology, Faculty of Agriculture, University of Zagreb, Zagreb, Croatia, 2018.
40. Abbas, A.F.; Ahmed, M.J. Mesoporous activated carbon from date stones (*Phoenix dactylifera* L.) by one-step microwave assisted K_2CO_3 pyrolysis. *J. Water Process Eng.* **2016**, *9*, 201–207. [CrossRef]
41. Bumajdad, A.; Khan, M.J.H.; Lukaszewicz, J.P. Nitrogen-enriched activated carbon derived from plant biomasses: A review on reaction mechanism and applications in wastewater treatment. *Front. Mater.* **2023**, *10*, 1218028. [CrossRef]
42. Bakshi, S.; Banik, C.; Laird, D.A. Estimating the organic oxygen content of biochar. *Sci. Rep.* **2020**, *10*, 13082. [CrossRef]
43. Tellez-Juárez, M.C.; Fierro, V.; Zhao, W.; Fernández-Huerta, N.; Izquierdo, M.T.; Reguera, E.; Celzard, A. Hydrogen storage in activated carbons produced from coals of different ranks: Effect of oxygen content. *Int. J. Hydrogen Energy* **2014**, *39*, 4996–5002. [CrossRef]

44. Zeng, Y.; Prasetyo, L.; Nguyen, V.T.; Horikawa, T.; Do, D.D.; Nicholson, D. Characterization of oxygen functional groups on carbon surfaces with water and methanol adsorption. *Carbon* **2015**, *81*, 447–457. [CrossRef]
45. Andas, J.; Rahman, M.L.A.; Yahya, M.S.M. Preparation and characterization of activated carbon from palm kernel shell. In *IOP Conference Series: Materials Science and Engineering*; IOP Publishing: Bristol, UK, 2017; Volume 226, p. 012156.
46. Jayakumar, M.; Hamda, A.S.; Abo, L.D.; Daba, B.J.; Venkatesa Prabhu, S.; Rangaraju, M.; Jabesa, A.; Periyasamy, S.; Suresh, S.; Baskar, G. Comprehensive Review on Lignocellulosic Biomass Derived Biochar Production, Characterization, Utilization and Applications. *Chemosphere* **2023**, *345*, 140515. [CrossRef]
47. González-García, P. Activated carbon from lignocellulosics precursors: A review of the synthesis methods, characterization techniques and applications. *Renew. Sustain. Energy Rev.* **2018**, *82*, 1393–1414. [CrossRef]
48. Correa, C.R.; Otto, T.; Kruse, A. Influence of the biomass components on the pore formation of activated carbon. *Biomass Bioenergy* **2017**, *97*, 53–64. [CrossRef]
49. Wanprakhon, S.; Sukcharoen, P.; Krongchai, S. A comparative study of one–step and two–step activated carbon from longan seeds by dry chemical activation with NaOH. *J. Mater. Sci. Appl. Energy* **2022**, *11*, 9–15. [CrossRef]
50. Kanikonna, K. Significance of Bacteria in Various Ecological Processes. *Appl. Microbiol. Open Access* **2023**, *9*, 1–2.
51. André, A.C.; Debande, L.; Marteyn, B.S. The selective advantage of facultative anaerobes relies on their unique ability to cope with changing oxygen levels during infection. *Cell Microbiol.* **2021**, *23*, e13338. [CrossRef] [PubMed]
52. Crone, S.; Vives-Flórez, M.; Kvich, L.; Saunders, A.M.; Malone, M.; Nicolaisen, M.H.; Martinez-Garcia, E.; Rojas-Acosta, C.; Gomez-Puerto, M.C.; Calum, H.; et al. The environmental occurrence of Pseudomonas aeruginosa. *APMIS* **2019**, *128*, 220–231. [CrossRef] [PubMed]
53. Armbruster, C.E.; Mobley, H.L.; Pearson, M.M. Pathogenesis of Proteus mirabilis infection. *EcoSal Plus* **2018**, *8*, 10–1128. [CrossRef] [PubMed]
54. Wareth, G.; Neubauer, H. The Animal-foods-environment interface of Klebsiella pneumoniae in Germany: An observational study on pathogenicity, resistance development and the current situation. *Vet. Res.* **2021**, *52*, 16. [CrossRef]
55. Fernández-Delgado, M.; Duque, Z.; Rojas, H.; Suárez, P.; Contreras, M.; García-Amado, M.A.; Alciaturi, C. Environmental scanning electron microscopy analysis of Proteus mirabilis biofilms grown on chitin and stainless steel. *Ann. Microbiol.* **2015**, *65*, 1401–1409. [CrossRef] [PubMed]
56. Howard, A.; O'Donoghue, M.; Feeney, A.; Sleator, R.D. *Acinetobacter baumannii*: An emerging opportunistic pathogen. *Virulence* **2012**, *3*, 243–250. [CrossRef]
57. Roy, R.; Tiwari, M.; Donelli, G.; Tiwari, V. Strategies for combating bacterial biofilms: A focus on anti-biofilm agents and their mechanisms of action. *Virulence* **2018**, *9*, 522–554. [CrossRef]
58. Jang, J.; Hur, H.G.; Sadowsky, M.J.; Byappanahalli, M.N.; Yan, T.; Ishii, S. Environmental Escherichia coli: Ecology and public health implications—A review. *J. Appl. Microbiol.* **2017**, *123*, 570–581. [CrossRef]
59. Reasoner, D.J. Microbiological Studies of Granular Activated Carbon Point-Of-Use. In Proceedings of the Conference on Point-of-Use Treatment of Drinking Water, Cincinnati, OH, USA, 6–8 October 1987; Water Engineering Research Laboratory, Office of Research and Development, US Environmental Protection Agency: Washington, DC, USA, 1988; p. 81.
60. Wang, G.; Zhao, G.; Chao, X.; Xie, L.; Wang, H. The characteristic of virulence, biofilm and antibiotic resistance of Klebsiella pneumoniae. *Int. J. Environ. Res. Public Health* **2020**, *17*, 6278. [CrossRef]
61. Yu, S.; Zhu, X.; Zhou, J.; Cai, Z. Biofilm inhibition and pathogenicity attenuation in bacteria by Proteus mirabilis. *R. Soc. Open Sci.* **2018**, *5*, 170702. [CrossRef]
62. Spector, M.P.; Kenyon, W.J. Resistance and survival strategies of Salmonella enterica to environmental stresses. *Food Res. Int.* **2012**, *45*, 455–481. [CrossRef]
63. Piletić, K.; Kovač, B.; Planinić, M.; Vasiljev, V.; Karačonji, I.B.; Žigon, J.; Gobin, I.; Oder, M. Combined biocidal effect of gaseous ozone and citric acid on acinetobacter baumannii biofilm formed on ceramic tiles and polystyrene as a novel approach for infection prevention and control. *Processes* **2022**, *10*, 1788. [CrossRef]
64. Guerreiro-Tanomaru, J.M.; de Faria-Júnior, N.B.; Duarte, M.A.H.; Ordinola-Zapata, R.; Graeff, M.S.Z.; Tanomaru-Filho, M. Comparative analysis of Enterococcus faecalis biofilm formation on different substrates. *J. Endod.* **2013**, *39*, 346–350. [CrossRef] [PubMed]

Disclaimer/Publisher's Note: The statements, opinions and data contained in all publications are solely those of the individual author(s) and contributor(s) and not of MDPI and/or the editor(s). MDPI and/or the editor(s) disclaim responsibility for any injury to people or property resulting from any ideas, methods, instructions or products referred to in the content.